Faraday Effect Due to Excitons in $Cd_{1-x}Mn_xTe$ Films

Tsuyoshi KOYANAGI*, Kimio NAKAMURA**, Koji YAMANO*,
and Kakuei MATSUBARA*

(Received July 15, 1988)

Abstract

Theoretical investigation has been performed on the Faraday effect of $Cd_{1-x}Mn_xTe$ epitaxial films prepared by the ionized-cluster beam (ICB) deposition technique. Splitting energies and oscillator strengths of an exciton level are calculated by taking account of a nondegenerate second order perturbation. The wavelength dispersion of the calculated Faraday rotation spectra is compared with the experimental data of $Cd_{1-x}Mn_xTe$ films. This suggests that the Faraday rotation is closely related to the magneto-optical transitions to Zeeman splitting levels of exciton.

1. Introduction

The ternary compound $Cd_{1-x}Mn_xTe$ is referred to as a semimagnetic semiconductor or diluted magnetic semiconductor, which has properties of both ordinary semiconductors and magnetic semiconductors. This new ternary compound permits one to vary the band gap, the lattice constant, and the other physical properties by controlling the manganese concentration.[1)~4)] There has been considerably interest in the epitaxial film growth or the superlattice of $Cd_{1-x}Mn_xTe$, which were realized by molecular beam epitaxy (MBE)[5)~7)] or atomic layer epitaxy (ALE)[8)], from the point of view of these ternary nature. On the other hand, much attention to this compound has been attracted for its magneto-optical properties, that is, the Faraday rotation[9)] due to the strong spin exchange interaction between Mn^{2+} ions and carriers, and the magneto-optical devices, such as an optical isolator, have been developed.[10),11)]

Our preliminary experiments[12)~16)] indicated that the epitaxial growth of $Cd_{1-x}Mn_xTe$ films on a sapphire (0001) substrate and their multilayered structure were possible at low substrate temperatures by applying the ionized-cluster beam (ICB) deposition technique, and that many significant results could be obtained with respect to their magneto-optical properties. The films obtained in our experiments exhibited a large dispersion of the Faraday rotation near their band gap energy, depending on the manganese composition and temperature. Because of very large optical absorption of the bulk crystal near the band gap energy, as compared with the intensity of its Faraday effect, there is no investigation of the dispersion of the Faraday rotation of this material in detail.

In this paper, we will report some results of theoretical investigations on the

*Department of Electronics

**Graduate student, Department of Electronics

Faraday effect of $Cd_{1-x}Mn_xTe$ epitaxial films, prepared by the ionized-cluster beam (ICB) deposition technique. We calculated a splitting energy and an oscillator strength of an exciton level by taking account of a nondegenerate second order perturbation. The wavelength dispersion of the Faraday rotation spectra was also calculated from the Zeeman splitting of an exciton level under an external magnetic field, and was compared with the experimental results of $Cd_{1-x}Mn_xTe$ films.

2. Theoretical Calculation of Faraday Rotations of $Cd_{1-x}Mn_xTe$

2.1 Splitting energies of an exciton level in a magnetic field

The Faraday effect of $Cd_{1-x}Mn_xTe$ is attributed to a large Zeeman splitting of the exciton state due to the spin exchange interaction between the localized $3d$ electrons of Mn^{2+} ions and the conduction and valence electrons. This splitting can be calculated using the perturbation theory, taking account of the exchange interactions.[17)~22)] The exciton effective mass Hamiltonian $\mathcal{H}$ for the relative electron-hole motion in the presence of a magnetic field can be written as

$$\mathcal{H}=\mathcal{H}_S+\mathcal{H}_{Mn}+\mathcal{H}'. \tag{1}$$

In Eq. (1), $\mathcal{H}_S$ is the spherical symmetric part of the Hamiltonian :

$$\mathcal{H}_S=\frac{p^2}{2\mu_0}-\frac{e^2}{\varepsilon r}, \tag{2}$$

where p is the relative electron-hole momentum, r is the electron-hole distance, e is the electron charge, ε is the static dielectric constant, and μ_0 is related to the Luttinger parameter γ_1 by the following equation: $1/\mu_0=1/m_e^*+\gamma_1/m_0$, where m_e^* is the electron effective mass and m_0 is the free electron mass.

$\mathcal{H}_{Mn}$ is the Hamiltonian for the spin exchange interaction, and when the magnetic field is applied along to the <111> crystal axis, $\mathcal{H}_{Mn}$ has the form as[2),18)]

$$\mathcal{H}_{Mn}=\frac{xN_0<S>}{\sqrt{3}}\left[(\sigma_x+\sigma_y+\sigma_z)\ \alpha-\ (J_x+J_y+J_z)\ \frac{\beta}{3}\right], \tag{3}$$

where x is the manganese composition, N_0 is the number of unit cells per unit volume, $<S>$ is the thermal average of manganese spins, σ_x, σ_y, and σ_z are the effective spin-1/2 operators, J_x, J_y, and J_z are the effective spin-3/2 operators, and α and β are the exchange integrals for the conduction and valence bands, respectively. Both $\mathcal{H}_S$ and $\mathcal{H}_{Mn}$ are taken as the unperturbed part of the total Hamiltonian $\mathcal{H}$.

On the other hand, $\mathcal{H}'$ can be considered as a perturbation with respect to the $\mathcal{H}_S+\mathcal{H}_{Mn}$, and is given by[18)]

$$\mathcal{H}'=\mathcal{H}_d+\mathcal{H}_l+\mathcal{H}_q+\mathcal{H}_{exch}, \tag{4}$$

where $\mathcal{H}_d$ is the anisotropy Hamiltonian with a d-like symmetry, $\mathcal{H}_l$ and $\mathcal{H}_q$ are the linear and quadratic terms of $\mathcal{H}'$ in a magnetic field H, respectively,and $\mathcal{H}_{exch}$ is the Hamiltonian for the electoron-hole exchange interaction. When the magnetic field is applied along to the <111> axis, these Hamiltonians are given by[19)~21)]

$$\mathcal{H}_d=\left(\frac{1}{\mu_l}\right)\left[\frac{5p^2}{4}-\ (p_x^2J_x^2+p_y^2J_y^2+p_z^2J_z^2)\right]$$

$$-\left(\frac{1}{\sqrt{3}\,\mu_2}\right)\left[p_xp_y\{J_xJ_y\}+p_yp_z\{J_yJ_z\}+p_zp_x\ \{J_zJ_x\}\right], \tag{5}$$

$$\begin{aligned}\mathcal{H}_1=&\left(\frac{eH}{2\sqrt{3}\,c}\right)\left[\frac{1}{m_e^*}-\frac{\gamma_1}{m_0}-\frac{5}{2\mu_1}\right]\left[(z-y)\ p_x+(x-z)\,p_y+(y-x)\,p_z\right]\\&+\left(\frac{eH}{\sqrt{3}\,\mu_1 c}\right)\left[(z-y)\,p_xJ_x^2+(x-z)\,p_yJ_y^2+(y-x)\,p_zJ_z^2\right]\\&+\left(\frac{eH}{6\mu_2 c}\right)\left(\left[(x-z)\,p_x+(z-y)\,p_y\right]\{J_xJ_y\}+\left[(y-x)\,p_y+(x-z)\,p_z\right]\{J_yJ_z\}\right.\\&\left.+\left[(z-y)\,p_z+(y-x)\ p_x\right]\{J_zJ_x\}\right)\\&+\left(\frac{\mu_BH}{\sqrt{3}}\right)\left[-2\kappa\,(J_x+J_y+J_z)-2q\,(J_x^3+J_y^3+J_z^3)+g_c\,(\sigma_x+\sigma_y+\sigma_z)\right],\end{aligned} \tag{6}$$

$$\begin{aligned}\mathcal{H}_q=&\left(\frac{eH}{2\sqrt{3}\,c}\right)^2\left\{\left(\frac{1}{2\mu_0}+\frac{5}{4\mu_1}\right)\left[(z-y)^2+(x-z)^2+(y-x)^2\right]\right.\\&-\left(\frac{1}{\mu_1}\right)\left[(z-y)^2J_x^2+(x-z)^2J_y^2+(y-x)^2J_z^2\right]\\&-\left(\frac{1}{\sqrt{3}\,\mu_2}\right)\left[(z-y)\,(x-z)\,\{J_xJ_y\}+(x-z)\,(y-x)\,\{J_yJ_z\}\right.\\&\left.\left.+(y-x)\,(z-y)\,\{J_zJ_x\}\right]\right\},\end{aligned} \tag{7}$$

$$\mathcal{H}_{exch}=\Delta_0+\Delta_1\,(\sigma_xJ_x+\sigma_yJ_y+\sigma_zJ_z)+\Delta_2\,(\sigma_xJ_x^3+\sigma_yJ_y^3+\sigma_zJ_z^3), \tag{8}$$

where γ_2, γ_3, κ, and q are the Luttinger parameters, c is the light velocity, μ_B is the Bohr magneton, g_c is the g factor of the conduction electron, and $\{ab\}=(ab+ba)/2$. The masses μ_1 and μ_2 are related to the Luttinger parameters γ_2 and γ_3, respectively, by the following equations : $1/\mu_1=\gamma_2/m_0$ and $1/\mu_2=2\sqrt{3}\,\gamma_3/m_0$.

$\mathcal{H}_{Mn}$ distinguishes the exchange contributions unambiguously from other aspects of

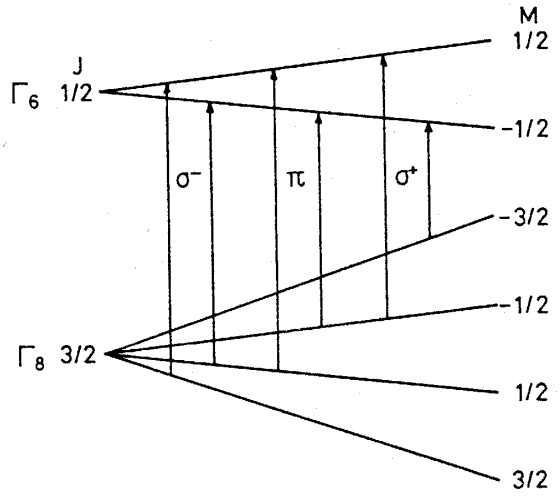

Fig. 1 Splitting pattern of conduction (Γ_6) and valence (Γ_8) bands of $Cd_{1-x}Mn_xTe$ in a magnetic field.

semiconductive behaviors that are non magnetic in origin, and influences an exciton level of $Cd_{1-x}Mn_xTe$. Figure 1 shows the splitting pattern of the Γ_6 conduction and Γ_8 valence bands of $Cd_{1-x}Mn_xTe$ in a magnetic field. The Γ_6 conduction band splits into two states ($\pm 3A$) and the Γ_8 valence band into four states ($\pm B$, $\pm 3B$) due to the exchange interaction.[17] The energies A and B of above Zeeman splittings are given by

$$A=\frac{xN_0<S>\alpha}{6}=\frac{M\alpha}{6g_{Mn}\mu_B},$$
$$B=\frac{xN_0<S>\beta}{6}=\frac{M\beta}{6g_{Mn}\mu_B}, \tag{9}$$

and depend on the magnetization M. In Eqs. (9), g_{Mn} is the g factor of Mn^{2+} ion.

$Cd_{1-x}Mn_xTe$ ($x<0.77$) exhibits a paramagnetic behavior, and its magnetic susceptibility χ is described by the Curie-Weiss law : [23]

$$M=xH=\frac{C_0x}{T+\Theta x}H, \tag{10}$$

where T is the absolute temperature. In this equation, the Curie constant C_0x and Curie temperature Θx are in proportion to the manganese composition x. From Eqs. (9) and (10), it is found that the Zeeman splitting energies of the conduction and valence bands vary depending on the manganese composition x and temperature T.

The eigenstates of the unperturbed part $\mathcal{H}_s+\mathcal{H}_{Mn}$ can be written as

$$|nlmi>=|nlm>|i>=|nlm>|\mu>|\sigma>, \tag{11}$$

where $|nlm>$ are the hydrogen wave functions, which are classified with the principal quantum number n, the azimuthal quantum number l, and the magnetic quantum number m (for the continuum state, n is replaced by $-i/k$, where k is the wave vector), and μ and σ are the eigenvalues of the spin operator J and σ, respectively. The energies E_{0i} and selection rules of the grand states $|100i>$ ($1s$ exciton), which are obtained from the unperturbed part of the total Hamiltonian $\mathcal{H}$, are summarized in Table 1. In this table, R_0 is the effective Rydberg energy, $R_0=\mu_0e^4/2\hbar^2\varepsilon^2$, where $\hbar$ is the Plank constant. The symbols "π", "σ^+", and "σ^-" mean the allowed magneto-optical transitions for the longitudinal polarization in the Voigt configuration and the right- and left- circular polarization in the Faraday configuration, respectively, and the symbol "$-$" means the forbidden transition.

Since the conduction and valence bands split due to the Hamiltonian $\mathcal{H}_{Mn}$, the $1s$ exciton states can be calculated by means of the second order nondegenerate theory.

Table 1 Energies and selection rules of the unperturbed exciton states.

i	Transition	Energy	Polarization
1	$\|3/2>_v\rightarrow\|1/2>_c$	$-R_0-3B+3A$	σ^-
2	$\|3/2>_v\rightarrow\|-1/2>_c$	$-R_0-3B-3A$	$-$
3	$\|1/2>_v\rightarrow\|1/2>_c$	$-R_0-B+3A$	π
4	$\|1/2>_v\rightarrow\|-1/2>_c$	$-R_0-B-3A$	σ^-
5	$\|-1/2>_v\rightarrow\|1/2>_c$	$-R_0+B+3A$	σ^+
6	$\|-1/2>_v\rightarrow\|-1/2>_c$	$-R_0+B-3A$	π
7	$\|-3/2>_v\rightarrow\|1/2>_c$	$-R_0+3B+3A$	$-$
8	$\|-3/2>_v\rightarrow\|-1/2>_c$	$-R_0+3B-3A$	σ^+

The energy E_i of the ith ($|100i>$) exciton level is given by

$$E_i = E_{0i} + <100i|\mathcal{H}'|100i> + \sum_i \mathrm{S}_n \frac{|<100i|\mathcal{H}'|nlmi>|^2}{E_{0i}-E_{ni}}, \tag{12}$$

where the symbol "S" means summations over discrete states and integrations over continuum states, and E_{ni} is the following eigenvalue for the $|nlmi>$ state :

$$E_{ni} = -R_0/n^2 + E_{0i} + R_0. \tag{13}$$

When the magnetic field is applied along to the $<111>$ crystal axis, we can write the energies E_i of the $1s$ exciton levels for the magneto-optical transitions in the Faraday configuration without respect to the electron-hole exchange interaction $\mathcal{H}_{\mathrm{exch}}$ as follows :

$$\begin{aligned}
E_1 &= -R_0 - 3B + 3A + \frac{g_c\mu_B H}{2\sqrt{3}} - \{[aS(0) + 4bS(2B) + 2cS(4B)] \\
&+ \frac{\gamma}{\sqrt{3}}\left[\frac{3\kappa\mu_0}{m_0} - 4bM(2B) - dM(4B)\right] \\
&+ \gamma^2\left[-\frac{1}{2} + \frac{aN(0)}{2} + 2bN(2B) + cN(4B) + \frac{aW(0)}{6}\right. \\
&\left. - \frac{2bW(2B)}{3} + \frac{cW(4B)}{3}\right]\}R_0, \\
E_4 &= -R_0 - B - 3A - \frac{g_c\mu_B H}{2\sqrt{3}} - \{[aS(0) + 4bS(-2B) + 2cS(4B)] \\
&+ \frac{\gamma}{\sqrt{3}}\left[\frac{\kappa\mu_0}{m_0} + 4bM(-2B) - dM(4B)\right] \\
&+ \gamma^2\left[-\frac{1}{2} + \frac{aN(0)}{2} + 2bN(-2B) + cN(4B) + \frac{aW(0)}{6} + \frac{2bW(2B)}{3}\right. \\
&\left. + \frac{cW(4B)}{3}\right]\} R_0, \\
E_5 &= -R_0 + B + 3A + \frac{g_c\mu_B H}{2\sqrt{3}} - \{[aS(0) + 4bS(2B) + 2cS(-4B)] \\
&+ \frac{\gamma}{\sqrt{3}}\left[-\frac{\kappa\mu_0}{m_0} - 4bM(2B) + dM(-4B)\right] \\
&+ \gamma^2\left[-\frac{1}{2} + \frac{aN(0)}{2} + 2bN(2B) + cN(-4B) + \frac{aW(0)}{6} - \frac{2bW(2B)}{3}\right. \\
&\left. + \frac{cW(-4B)}{3}\right]\}R_0, \\
E_8 &= -R_0 + B - 3A - \frac{g_c\mu_B H}{2\sqrt{3}} - \{[aS(0) + 4bS(-2B) + 2cS(-4B)] \\
&+ \frac{\gamma}{\sqrt{3}}\left[-\frac{3\kappa\mu_0}{m_0} + 4bM(-2B) + dM(-4B)\right] \\
&+ \gamma^2\left[-\frac{1}{2} + \frac{aN(0)}{2} + 2bN(-2B) + cN(-4B) + \frac{aW(0)}{6} - \frac{2bW(-2B)}{3}\right. \\
&\left. + \frac{cW(-4B)}{3}\right]\}R_0,
\end{aligned} \tag{14}$$

$$a=\frac{16}{5}\left(\frac{\mu_0}{\mu_1}\right)^2,$$

$$b=\frac{2}{15}\left(\frac{\mu_0}{\mu_2}\right)^2,$$

$$c=\frac{2}{5}\left[4\left(\frac{\mu_0}{\mu_1}\right)^2\frac{1}{3}\left(\frac{\mu_0}{\mu_2}\right)^2\right],$$

$$d=\frac{32\sqrt{3}}{15}\left(\frac{{\mu_0}^2}{\mu_1\mu_2}\right),$$

where γ is the ratio of the cyclotron energy to the double Rydberg energy, that is, $\gamma=e\hbar H/2\mu_0 R_0$. In this calculation, the term of $\mathcal{H}_1$ Hamiltonian proportional to the Luttinger parameter q is neglected. The functions S, M, N, and W in Eqs. (14) are given by[18]

$$\begin{aligned}
S(y)&=\sum_{n=3}^{\infty}\frac{|I_n|^2}{y+1-1/n^2}+\int_0^{\infty}\frac{|I_k|^2}{y+1+k^2}dk,\\
N(y)&=\sum_{n=3}^{\infty}\frac{|L_n|^2}{y+1-1/n^2}+\int_0^{\infty}\frac{|L_k|^2}{y+1+k^2}dk,\\
M(y)&=\sum_{n=3}^{\infty}\frac{L_nI_n}{y+1-1/n^2}+\int_0^{\infty}\frac{L_kI_k}{y+1+k^2}dk,\\
W(y)&=\sum_{n=3}^{\infty}\frac{I_nH_n}{y+1-1/n^2}+\int_0^{\infty}\frac{I_kH_k}{y+1+k^2}dk,
\end{aligned}\tag{15}$$

where I_n, I_k, L_n, L_k, H_n, and H_k are integrals of radial hydrogen-like functions multiplied by some powers of r.[19)~21)]

The Hamiltonian $\mathcal{H}_{\text{exch}}$ for the electron-hole exchange interaction plays an important role in the splitting of the exciton level at low magnetic fields and high temperatures. In the present analysis, we neglect terms in $\mathcal{H}_{\text{exch}}$ that include Δ_2. The basis of the eigenstates of I diagonalizes $\mathcal{H}_{\text{exch}}$, where I is the eigenvalue of the exciton total angular momentum. These eigenstates can be denoted by $|I, M>$, where M is the projection of I on the quantization axis along to the magnetic field H. The relationship between $|i>=|\mu>|\sigma>$ and $|I, M>$ basis can be described using the Clebsch-Gordan coefficients.[18),21)] In the absence of a magnetic field, $I=1$ states are visible in σ^+ ($M=+1$), σ^- ($M=-1$), and π ($M=0$) polarizations, but $I=2$ states are forbidden.

When $\mathcal{H}'$ are diagonalized in the basis $|I, M>$, the following energies $E_I^{\pm}$ ($M=+1$ for the upper sign $+$ and $M=-1$ for the lower sign $-$) of the exciton levels for the σ polarization are obtained :

$$\begin{aligned}
E_1^-&=\frac{1}{2}\left[E_1+E_4+2\Delta_0+\frac{\Delta_1}{2}+\sqrt{(E_1-E_4+\Delta_1)^2+3{\Delta_1}^2}\right]+E_g, && \sigma_1^-\\
E_1^+&=\frac{1}{2}\left[E_5+E_8+2\Delta_0+\frac{\Delta_1}{2}+\sqrt{(E_8-E_5+\Delta_1)^2+3{\Delta_1}^2}\right]+E_g, && \sigma_1^+\\
E_2^-&=\frac{1}{2}\left[E_1+E_4+2\Delta_0+\frac{\Delta_1}{2}-\sqrt{(E_1-E_4+\Delta_1)^2+3{\Delta_1}^2}\right]+E_g, && \sigma_2^-\\
E_2^+&=\frac{1}{2}\left[E_5+E_8+2\Delta_0+\frac{\Delta_1}{2}-\sqrt{(E_8-E_5+\Delta_1)^2+3{\Delta_1}^2}\right]+E_g, && \sigma_2^+
\end{aligned}\tag{16}$$

where E_g is the band gap energy, which depends on the manganese composition and

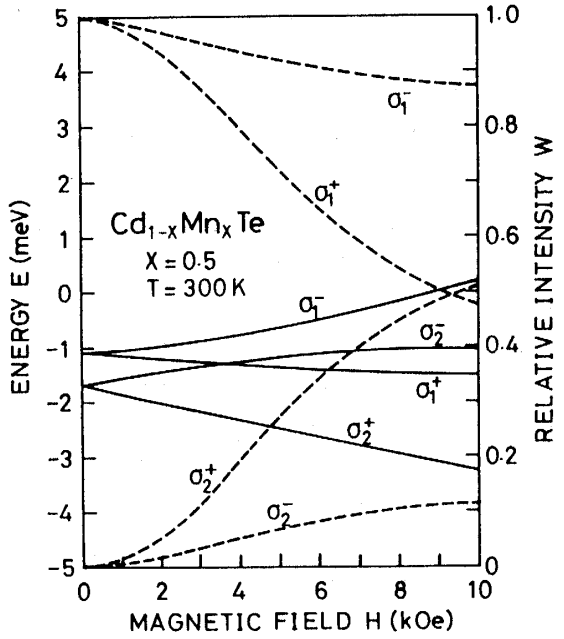

Fig. 2 Magnetic field dependences of the splitting energies (solid line) and relative oscillator strengths (dashed line) of the exciton states in $Cd_{1-x}Mn_xTe$.

temperature.[24]

The presence of $\mathcal{H}_{exch}$ influences the relative oscillator strengths of the transitions to exciton levels. The relative oscillator strenghts $W_I^{\pm}$ can be obtained from Eq. (14) :

$$W_1^- = 8|p_0|^2 3\left[\frac{1}{2} + \frac{2b_1}{3+4(1/2+b_1)^2}\right], \quad \sigma_1^-$$

$$W_1^+ = 8|p_0|^2 3\left[\frac{1}{2} + \frac{2b_2}{3+4(1/2+b_2)^2}\right], \quad \sigma_1^+$$

$$W_2^- = 8|p_0|^2\left[\frac{1}{2} - \frac{6b_1}{3+4(1/2+b_1)^2}\right], \quad \sigma_2^- \qquad (17)$$

$$W_2^+ = 8|p_0|^2\left[\frac{1}{2} - \frac{6b_2}{3+4(1/2+b_2)^2}\right], \quad \sigma_2^+$$

$$b_{1,2} = a_{1,2} + \sqrt{1+a_{1,2}+a_{1,2}^2},$$

$$a_1 = \frac{E_1 - E_4}{2|\Delta_1|},$$

$$a_2 = \frac{E_8 - E_5}{2|\Delta_1|},$$

where p_0 is the momentum matrix element for the transition between Γ_6 conduction and Γ_8 valence bands.

Figure 2 shows the magnetic field dependences of the splitting energies and relative oscillator strengths of the exciton levels for the σ polarization, which were calculated from Eqs. (16) and (17). The values of parameters used in these calculations are summarized in Table 2, and the values of p_0, the Luttinger parameters, and the other parameters were estimated in terms of the semiempirical model based on the $k \cdot p$ perturbation theory, which was proposed by Lawaetz.[26] From this figure, it was found

that the exciton level split into two due to the electron-hole exchange interaction in the absence of a magnetic field, and that the Zeeman splitting energies of the exciton levels increased with increasing the magnetic field. The Zeeman splitting energy is anomalously large compared with ordinary semiconductors. For example, the values of the splitting energies at $x=0.5$, $T=300$K, and $H=10$kOe are larger approximately thirty times for the σ_1 polarization and forty times for σ_2 than those of CdTe, which is a nonmagnetic parent crystal for $Cd_{1-x}Mn_xTe$. When the magnetic field is present, the transitions for σ_2 polarization are allowed, and their oscillator strengths are enhanced with the magnetic field.

Figure 3 shows the calculated results of the manganese composition dependences of the splitting energies and relative oscillator strengths of the exciton levels for the σ polarization. The dependences tend to behave similarly to the magnetic field dependences. The exciton levels shift toward low energy sides, and their splittings are enhanced with increasing the manganese composition.

Table 2 Parameters used for the calculation.

$\alpha N_0=0.22$eV[25]	$\beta N_0=-0.88$eV[25]
$C_0/N_0=7.09\times10^{-24}$K/cm^3 [23]	$\Theta=470$K[23]
$\Delta_0=0.23$meV[18]	$\Delta_1=-0.30$meV[18]
$C=1.7\times10^{-3}$	
$\Gamma_1=250$meV (300K)	$\Gamma_2=150$meV (300K)
$\Gamma_1=175$meV (100K)	$\Gamma_2=140$meV (100K)

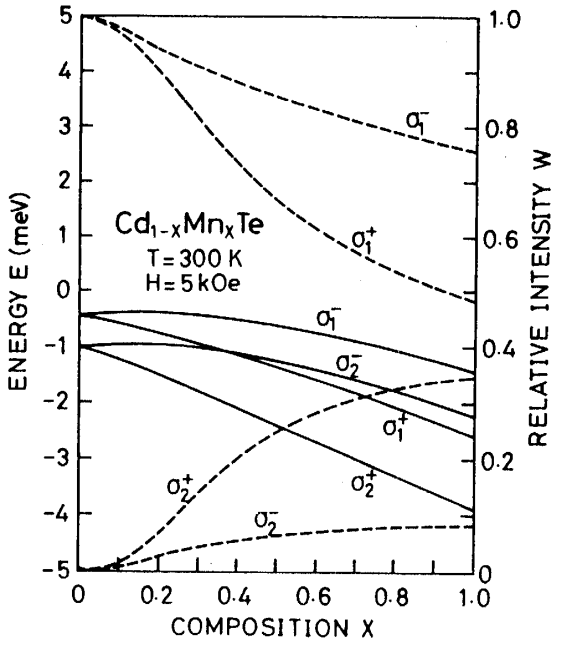

Fig. 3 Manganese composition dependences of the splitting energies (solid line) and relative oscillator strengths (dashed line) of the exciton states in $Cd_{1-x}Mn_xTe$.

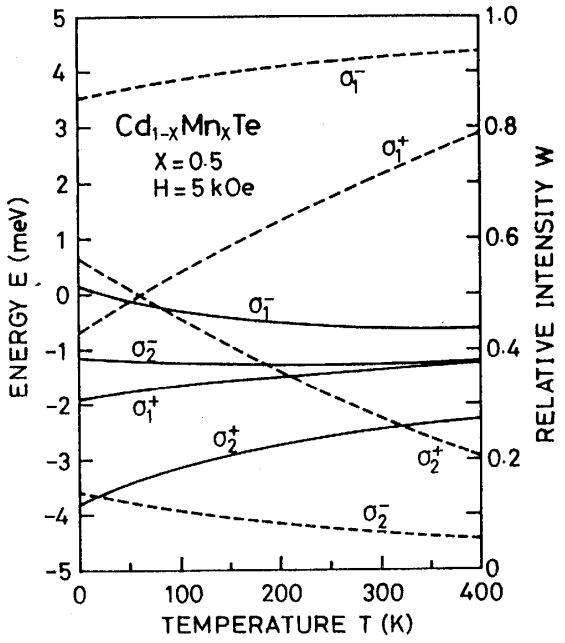

Fig. 4 Temperature dependences of the splitting energies (solid line) and relative oscillator strengths (dashed line) of the exciton states in $Cd_{1-x}Mn_xTe$.

The splittings of exciton levels of $Cd_{1-x}Mn_xTe$ strongly depend on the temperature through the magnetization M. Figure 4 shows the dependences of the splitting energies and relative oscillator strengths of the exciton levels for the σ polarization. The splitting energies increase with lowering the temperature. These dependences for the magneto-optical transitions to exciton levels are closely related to the magnetization M depending on the magnetic field, manganese composition, and temperature through the spin exchange interaction $\mathcal{H}_{Mn}$.

2.2 Faraday rotation due to the exciton effect

The Faraday rotation θ_F of $Cd_{1-x}Mn_xTe$ can be obtained from the difference between the refractive indices $n^{\pm}$ for the right- and left-circular polarization by

$$\theta_F(E)=\frac{E}{2\hbar c}[n^-(E)-n^+(E)]. \tag{18}$$

In order to calculate the refractive indices $n^{\pm}$, the dispersion of the complex dielectric constants $\varepsilon^{\pm}$ for the magneto-optical transitions to exciton levels is required. We assume a classical damped oscillator model,[27]

$$\varepsilon^{\pm}(E)=\varepsilon_{\infty}+\sum_I \frac{4\pi\beta_I^{\pm}}{E_I^{\pm 2}-E^2+iE\Gamma_I}, \tag{19}$$

where $4\pi\beta_I^{\pm}$ are the oscillator strengths, which are in proportion to the relative oscillator strengths calculated from Eq. (17) (i. e. $4\pi\beta_I^{\pm}=CW_I^{\pm}$, C : constant), $E_I^{\pm}$ are the energies of exciton levels calculated from Eq. (16), and Γ_I is a temperature dependent damping constant. In Eq. (19), it is assumed that the value of ε_{∞} for any manganese compositions is equal to 7.21 for CdTe.[28] We neglect the contribution of

the interband Faraday rotation to the dispersion of the Faraday rotation, because the Faraday rotation due to the interband effect is considerably small at the band gap energy, as compared with that due to the exciton effect. The constants C and Γ_I were adjusted to fit the calculated dispersion spectra of Faraday rotations to the experimental results.

3. Results and Discussions

The $Cd_{1-x}Mn_xTe$ epitaxial films used in measurements of Faraday rotation spectra were prepared on a sapphire (0001) substrate by applying the ionized-cluster beam deposition technique.[13] The obtained films were grown epitaxially along to the <111> axis perpendicular to the substrate plane, and their thicknesses were of $\sim 1\mu$m. Measurements of the Faraday rotation were performed under applying the magnetic field of 5kOe, perpendicular to the film plane, at liquid nitrogen and room temperatures in the wavelength region from 800 to 450nm.

Figure 5 shows the dispersion spectra of the Faraday rotation θ_F for $Cd_{1-x}Mn_xTe$ films with different compositions. The parameters C and Γ_I used for these calculations were independent of the manganese composition, as summarized in Table 2. In this figure, the calculated spectra are in good agreement with the experimental results, except for the oscillations of the Faraday rotation at low energy sides of the dispersions caused by the interference fringe in the films. For the film with $x=0.77$, a small dispersion is observed at 2.3eV due to the $d-d$ transition of Mn^{2+} ions,[29] and the peak height of the main dispersion is slightly small compared with the theoretical curve. This disagreement is attributed to the reduction of the Zeeman splitting at high x values, which can be explained in terms of a second order correction to the molecular field formula.[30]

Figure 6 shows the Faraday rotation spectra of the $Cd_{1-x}Mn_xTe$ film with $x=0.21$ at $T=100$ and 300K. The calculated spectra agree satisfactorily with the experimental results at both temperatures using the suitable parameters C and Γ_I. The shift of the

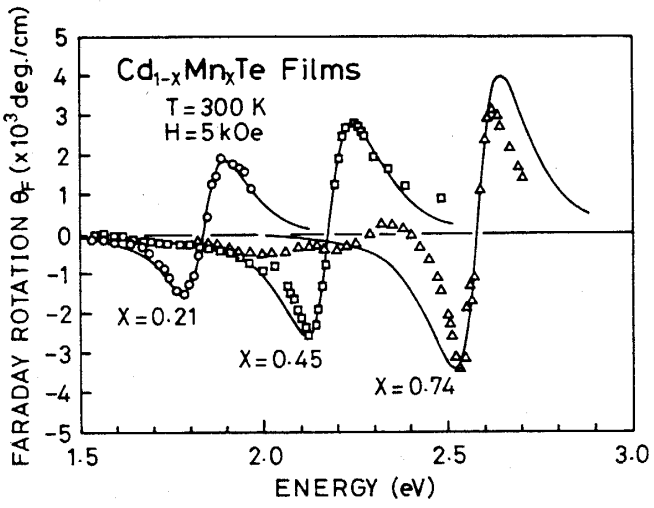

Fig. 5 Faraday rotation spectra of the $Cd_{1-x}Mn_xTe$ films with the different compositions at room temperature. Solid lines indicate the calculated spectra.

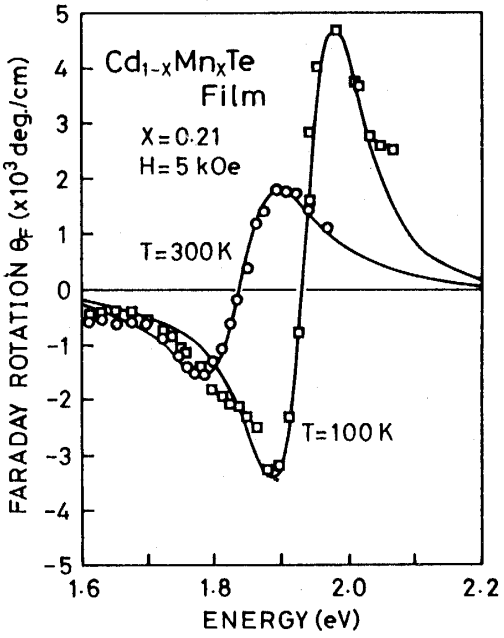

Fig. 6 Faraday rotation spectra of the $Cd_{1-x}Mn_xTe$ ($x=0.21$) film at different temperatures. Solid lines indicate the calculated spectra.

dispersion toward higher energies at low temperature is caused by the temperature dependence of the band gap energy.

4. Conclusion

The dispersion spectra of the Faraday rotation of $Cd_{1-x}Mn_xTe$ films, prepared by the ICB deposition technique, were calculated theoretically from the splittings of exciton levels using the nondegenerate second order perturbation theory, and the results were compared with the experimental results. The Zeeman splittings are enhanced with increasing the manganese composition, lowering the temperature, and applying the magnetic field through the magnetization with the Curie-Weiss behavior. The exciton level splits into eight levels, which correspond to six allowed magneto-optical transitions for two π and four σ polarizations and two forbidden transitions. The Faraday rotation spectra calculated from the transition energies to these exciton levels and their oscillator strengths are in good agreement with the experimental results at different compositions and temperatures. From these results, it was found that the exciton effect was important for the Faraday rotation of $Cd_{1-x}Mn_xTe$.

REFERENCES

1) R. R. Galazka, Inst. Phys. Conf. Ser., No. **43**, 133 (1979).
2) J. K. Furdyna, J. Appl. Phys., **53**, 7637 (1982).
3) N. B. Brandt and V. V. Moshchalkov, Adv. Phys., **33**, 193 (1984).
4) O. Godede and W. Heimbrodt, Phys.Status Solidi b, **146**, 11 (1988).

5) L. A. Kolodziejski, T. Sakamoto, R. L. Gunshor, and S. Datta, Appl. Phys. Lett., **44**, 799 (1984).
6) L. A. Kolodziejski, T. C. Bonsett, R. L. Gunshor, S. Datta, R. B. Bylsma, W. M. Becker, and N. Otsuka, Appl. Phys. Lett., **45**, 440 (1984).
7) R. N. Bicknell, R. W. Yanka, N. C. Giles-Taylor, D. K. Blanks, E. L. Buckland, and J. F. Schetzina, Appl. Phys. Lett., **45**, 92 (1984).
8) M. Pessa and O. Jylhä, Appl. Phys. Lett., **45**, 646 (1984).
9) J. A. Gaj, R. R. Galazka, and M. Nawrocki, Solid State Commun., **25**, 193 (1978).
10) A. E. Turner, R. L. Gunshor, and S. Datta, Appl. Opt., **22**, 3152 (1983).
11) N. Kullendorff and B. Hök, Appl. Phys. Lett., **46**, 1016 (1985).
12) T. Koyanagi, Y. Obata, K. Matsubara, H.Takaoka, and T. Takagi, J. Magn. Soc. Jpn., **9**, 141 (1985).
13) T. Koyanagi, K. Matsubara, H. Takaoka, and T. Takagi, J. Appl. Phys., **61**, 3020 (1987).
14) T. Watanabe, K. Yamano, T. Koyanagi, and K. Matsubara, J. Magn. Soc. Jpn., **11**, 317 (1987).
15) T. Koyanagi, T. Watanabe, and K. Matsubara, IEEE Trans. Magn., **23**, 3214 (1987).
16) T. Koyanagi, K. Nakamura, K. Yamano, and K. Matsubara, J. Magn. Soc. Jpn., **12**, 187 (1988).
17) A. Twardowski, M. Nawrocki, and J. Ginter, Phys. Status Solidi b, **96**, 617 (1979).
18) M. Z. Cieplak, Phys. Status Solidi b, **97**, 617 (1980).
19) A. Baldereschi and N. O. Lipari, Phys. Rev. B, **3**, 439 (1971).
20) M. Altarelli and N. O. Lipari, Phys. Rev. B, **7**, 3798 (1973).
21) K. Cho, S. Suga, W. Dreybrodt, and F. Willmann, Phys. Rev. B, **11**, 1512 (1975).
22) L. Swierkowski, Il Nuovo Chimento B, **29**, 340 (1975).
23) J. Spalek, A. Lewicki, Z. Tarnawski, J. K. Furdyna, R. R. Galazka, and Z. Obuszko, Phys. Rev. B, **33**, 3407 (1986).
24) B. Montegu, A. Laugier, and R. Triboulet, J. Appl. Phys., **56**, 3061 (1984).
25) J. A. Gaj, R. Planel, and G. Fishman, Solid State Commun., **29**, 435 (1979).
26) P. Lawaetz, Phys. Rev. B, **4**, 3460 (1971).
27) S. Suga, T. Koda, and T. Mitani, Phys. Status Solidi b, **54**, 393 (1972).
28) D. T. F. Marple, J. Appl. Phys., **35**, 539 (1964).
29) N. T. Khoi and J. A. Gaj, Phys. Status Solidi b, **83**, K133 (1977).
30) J. P. Lascaray, D. Coquillat, J. Deporetes, and A. K. Bhattacharjee, Phys. Rev. B, to be published.